

We are IntechOpen, the world's leading publisher of Open Access books Built by scientists, for scientists

6,900

Open access books available

186,000

International authors and editors

200M

Downloads

Our authors are among the

154

Countries delivered to

TOP 1%

most cited scientists

12.2%

Contributors from top 500 universities



WEB OF SCIENCE™

Selection of our books indexed in the Book Citation Index
in Web of Science™ Core Collection (BKCI)

Interested in publishing with us?
Contact book.department@intechopen.com

Numbers displayed above are based on latest data collected.
For more information visit www.intechopen.com



Experimental Study of Flow-Induced Vibrations and Scattering of Roof Tiles by Wind Tunnel Testing

Satoru Okamoto
Shimane University
Japan

1. Introduction

The tremendous destruction caused by recent typhoons in Japan has caused a substantial upsurge in interest in the subject of global warming among news media and the wider public. There are concerns that global climate change may have played a significant role in these events. Some believe that global warming is responsible for an increase in the frequency of destructive natural events. Typhoons cause the destruction of tiles on the rooftops of Japanese residences. The wind load on a roofing element is created by the difference between the external and internal pressures. The net wind load is, in general, determined by the building flow field, wind gustiness, and the element flow field (Peterka et al, 1997; Cermak, 1998). Although these parameters directly influence the external pressure distribution on a roofing element, the development of internal pressure, which indirectly depends on these parameters, is governed by a dynamic response that varies according to different roofing elements. The pressure distribution on an external roof surface and internal pressure distribution have been determined in numerous studies (Hazelwood, 1980; Ginger, 2001). Element wind loading may differ significantly from the load derived from the external pressure distribution. Internal pressure is governed by the wind permeability of the surface, which is determined by openings, such as gaps between tiles or venting devices, and by the equilibrating resistance through and underneath a wind permeable surface (Kramer et al, 1979).



Fig. 1. Japanese residence and roof tiles

Flow-induced vibration of roof tiles usually appears just before they are scattered. The flow-induced vibration (aeroelastic instability) of structures is an important phenomenon for the following two reasons: (1) strong lateral self-excited oscillations can develop at a certain wind velocity (onset velocity) as a result of the lateral aerodynamic force component and (2) these vibrations have a tendency to affect the behavior of the structure prior to the onset velocity because they produce negative aerodynamic damping that can considerably reduce the total damping available to the structure (Naudascher et al., 1993). However, the flow-induced vibration of roof tiles prior to scattering has been given very little attention. This study investigates the nature and source of the vibrating and scattering behavior of the roof tiles in order to provide better insight into this mechanism. This paper presents the first results of studies on the wind-inducing mechanism in roof tiles, which are widely used for roofing Japanese wooden dwellings (Fig. 1).

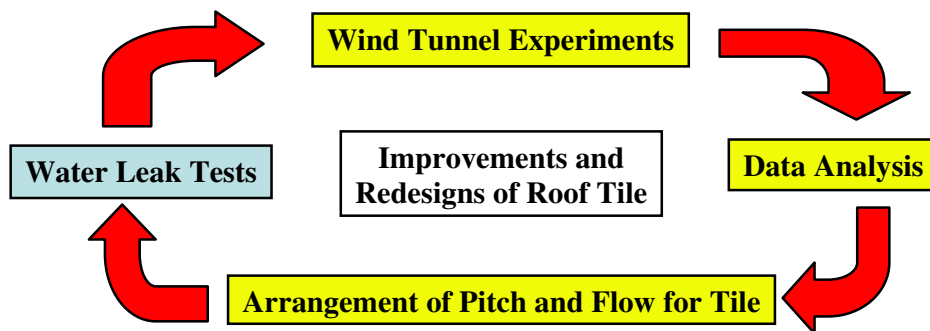


Fig. 2. Outline of the research

Using wind tunnel tests, an experimental study was conducted to explain the behavior of roof tile vibration and the primary factors that affect their scattering. The results indicate that the vibration mechanism behaves in a manner that is consistent with that of a self-excited system, and the surface flow creates reasonable up-lifting moments only when the wind direction is roughly perpendicular to that of the eaves (Fig. 2).

Nomenclature

- θ pitch angle (degree)
- ϕ flow angle (degree)
- U upstream flow velocity (m/s)
- X streamwise coordinate
- Y transverse coordinate
- Z coordinate perpendicular to the surface of a roof tile

2. Test facility and analysis procedure

Fig. 3 illustrates the general layout of the apparatus used in this experiment. The experiments were conducted in an open-circuit wind tunnel that was driven by an axial flow fan. The nozzle of the wind tunnel had a 500 mm × 1,300 mm cross section. The maximum velocity of flow from the nozzle was approximately 50.0 m/s. The representative wind velocity was measured by a hot-wire anemometer and a linearizer on the exit nozzle of the wind tunnel. Approximately 10.0% of the flow's streamwise turbulence intensity was

generated by the grids. The spatial characteristics of air jet were checked for uniformity in wind speed and turbulence to ensure that all tiles were exposed to a near uniform air flow. The turbulence intensity of the flow condition is of the same order as the turbulence intensity experienced in practice.

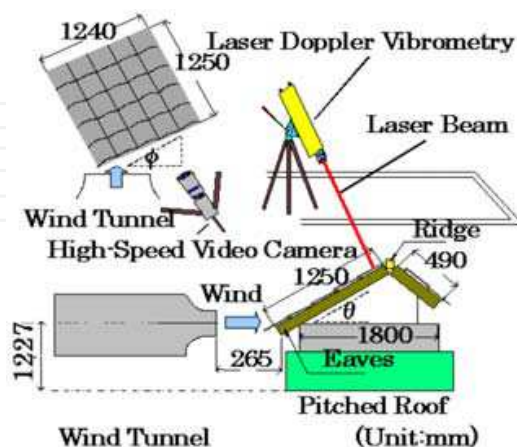
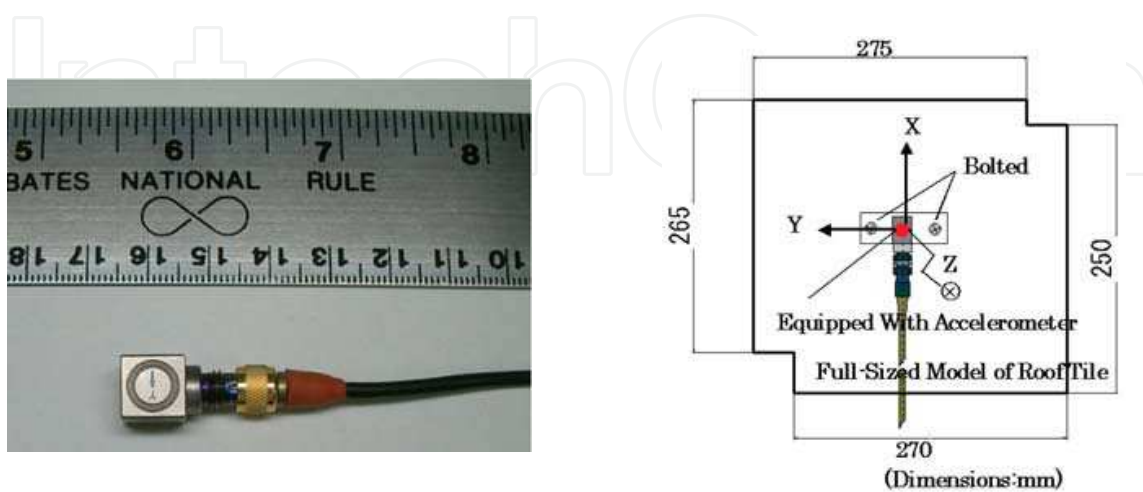


Fig. 3. Experimental apparatus

25 roof tiles were set up in 5 rows \times 5 columns on a pitched roof in the downstream flow of a wind tunnel (Fig. 3). The roof tiles were tested by the air flow, which barely covered the entire exposed area of the tiles. They were made of clay, and each weighed approximately 2.8 kg. The tiled pitched roof was fitted similar to a real roof arrangement with a plenum underneath the tiles, which acts as a roof cavity. This plenum was sealed with a clay pad. The internal pressure in this plenum was monitored and regulated by a pressure transducer placed underneath the tiles. The vibrations of the roof tiles were measured by a laser Doppler vibrometer (LDV, OMETRON VS1000) and an accelerometer (ONO SOKKI NP-3560, Fig. 4 (a)), and the normal natural frequencies of the roof tiles were analyzed using an impulse force hammer test. The vibration velocity could be measured up to 1,000 mm/s by a 1 mW LDV, and the range of the vibrational frequency was from 0 to 50 kHz. One roof tile was equipped with an accelerometer (Fig. 4 (b)). The accelerometer was used to measure the dynamic behavior of the tiles in three directions, X-, Y-, and Z under a no-flow condition,



(a) Accelerometer

b) Roof tile equipped with accelerometer

Fig. 4. Accelerometer used in the experiments

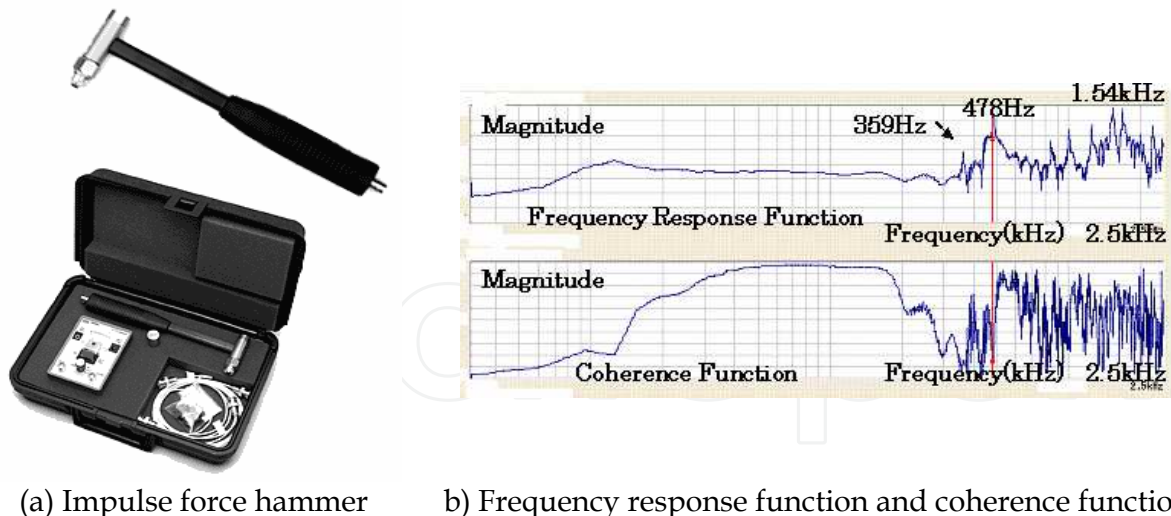


Fig. 5. Frequency response function and coherence function of a roof tile generated by an impulse force hammer test

and weighed approximately 5.0 g. The experimental measurement of the vibration frequencies for tiles was performed with the accelerometer. However, the vibration frequencies identified by the LDV were limited to small-amplitude modes. In this study, the accelerometer and LDV were used to determine the resonant frequencies of roof tiles that were and were not bolted to the roof bed.

An impact hammer with a force transducer was used to excite the tiles under no-flow conditions (Fig. 5 (a)). Two signal conditioners were used to provide power to the accelerometer and the force transducer, whose spectral analyses were performed using a fast Fourier transform (FFT) spectrum analyzer (ONO SOKKI DS-2100 4CH). The sampling frequency was 5,120 Hz over a frequency range of 0 - 2.5 kHz; 1,024 data points were sampled per spectrum. Unless otherwise stated, 64 spectra were averaged for each measurement. The frequency resolution of the spectra was 5 Hz. In order to analyze acceleration in a direction perpendicular to the surface of a roof tile, the time taken by the acceleration signal was recorded using the FFT analyzer. Two accelerometers were used simultaneously. Roof tiles that showed significant vibrations at any velocity, found from a series of experiments using accelerometers, were attached to two neighboring roof tiles on a model roof.

The dynamic instability of the structure under excitation was also visually investigated. Large amplitude vibrations and the scattering of roof tiles were observed by a high-speed video camera (PHOTRON FASTCAM-PCI 2KC). The images were acquired at 2,000- frames per second, at a resolution of 512 pixels \times 480 pixels per full frame. A hot-wire anemometer and a linearizer were used to measure the turbulence intensity of surface flow over the roof tiles.

3. Results and discussion

3.1 Impulse force hammer test for roof tiles

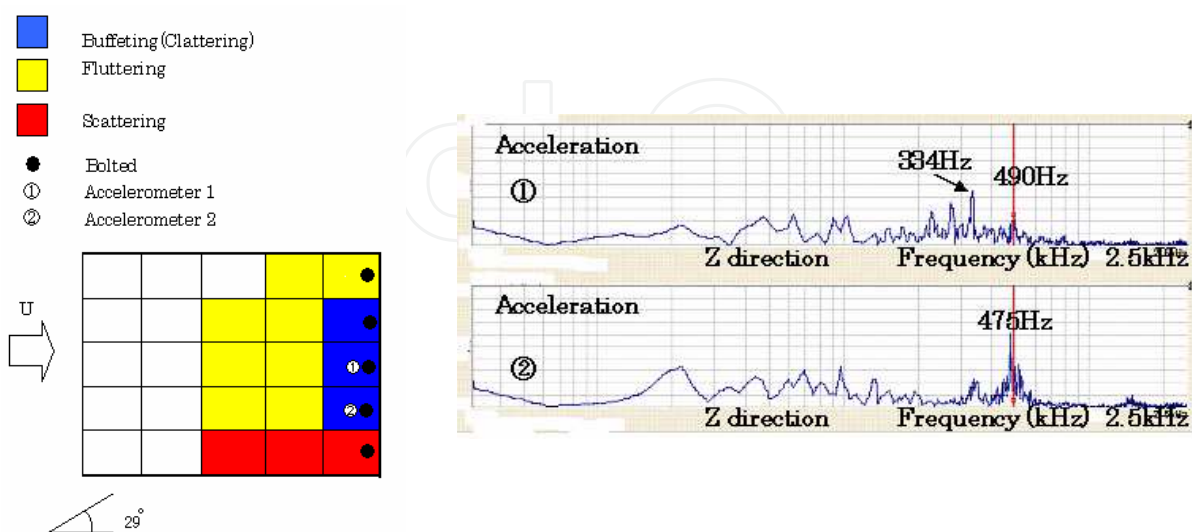
Fig. 5 (b) shows the frequency response function curve and coherence function curve of roof tiles measured using an impact hammer with a force transducer. One of the resonant frequencies obtained by the accelerometer was 478 Hz. As stated in the next section, the measured frequencies obtained using the wind tunnel test are nearly consistent with the resonant frequencies obtained by the excitation analysis of the impulse force hammer test.

The value of the input excitation level is set to be approximately constant for the excitation analysis. However, the flow-induced excitation level is amplified and a higher level should be provided to obtain vibration measurements. On the other hand, the variation in the measured values of resonant frequencies for the accelerometer measurement and excitation analysis may be attributed to the added weight of the accelerometer in this experimental technique. In order to eliminate the effect of the added weight of the accelerometer on the resonant frequencies of the roof tile, the corresponding frequency response curve of this roof tile was obtained using the LDV. The peak values of this frequency response curve were compared with those obtained using the accelerometer method. It was found that the results of resonant frequencies measured using LDV and those using the accelerometer agreed satisfactorily.

3.2 Acceleration measurements of roof tile

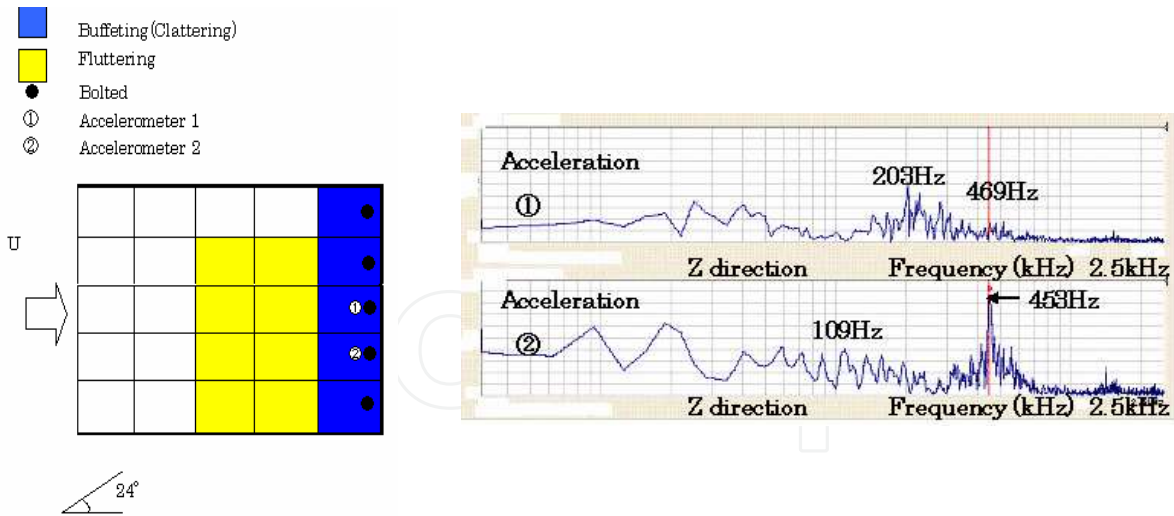
In the measurement and analysis of roof tile vibration and its acceleration, the pitch of the roof θ was set at 19 degrees, 24 degrees, and 29 degrees and the flow angle ϕ was set at 0 degrees. The wind velocity was gradually increased from 0 to 50.0 m/s or until scattering of the tiles occurred. The signals from the accelerometers were recorded to be analyzed later using a personal computer.

The slope angle of the roof was changed, and the effects of fluttering in the last stage of roof tile scattering were examined (Figs. 6-8). The small-amplitude vibration of the model roof tiles appeared in a low-velocity flow at the maximum pitch angle of 29 degrees, while the model roof tiles showed fluttering when the wind velocity reached approximately 38 m/s. They were more buffeted at the pitch angle of 24 degrees than at the pitch angle of 29 degrees, and then fluttered when the wind velocity reached approximately 40 m/s. The model roof tiles did not flutter at the minimum pitch angle of 19 degrees, and they were buffeted at a higher wind velocity than that at other pitch angles. They did not flutter at pitch angles of 24 and 29 degrees because of the weight of the neighboring roof tiles and bolts. The fluttering of the model roof tiles appeared with relatively large-amplitude vibrations, and it was regarded as fluttering when the roof tile was completely lifted from the roofing board and the board was exposed.



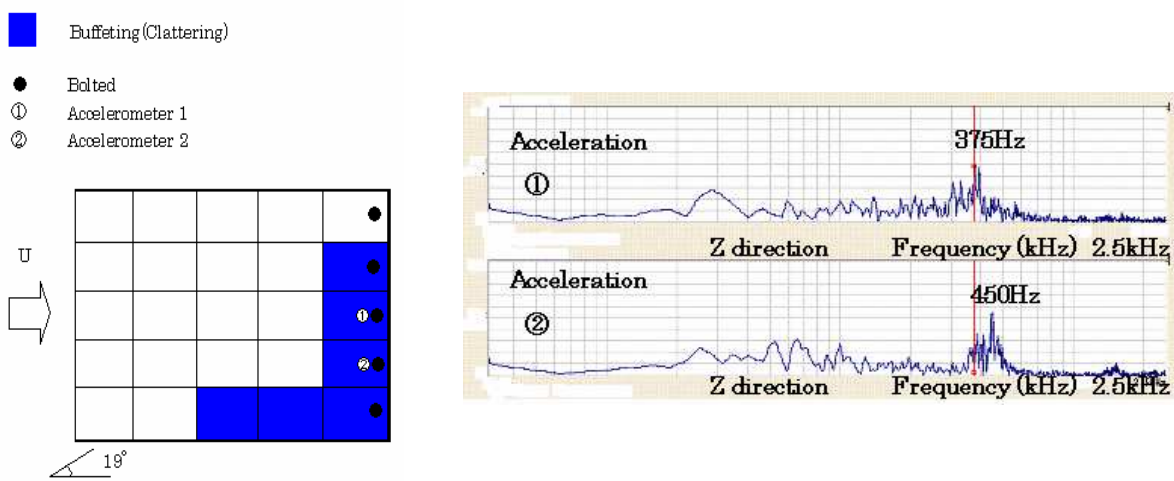
(a) Vibration of roof tiles b) Vibrational acceleration power spectrum for roof tiles

Fig. 6. Effect of slope angle of roof on vibration of roof tiles at $\theta = 29$ degrees, $U = 39.0$ m/s



(a) Vibration of roof tiles b) Vibrational acceleration power spectrum for roof tiles

Fig. 7. Effect of slope angle of roof on vibration of roof tiles at $\theta = 24$ degrees, $U = 38.5$ m/s



(a) Vibration of roof tiles b) Vibrational acceleration power spectrum for roof tiles

Fig. 8. Effect of slope angle of roof on vibration of roof tiles at $\theta = 19$ degrees, $U = 39.9$ m/s



Fig. 9. Observation of the flow on the surface of the roof tile by the oil film method

The occurrence of fluttering was considered as one of the last stages of roof tile scattering. Fluttering did not occur at the lower pitch angle and, as a result, the model roof tiles resisted vibration and scattering at even higher velocities, whereas fluttering occurred at a higher pitch angle because the model roof tiles were often buffeted and scattered by lower critical velocities. In addition, the oil-film method was used to observe the flow pattern on the surface of the every tile in the model roof (Fig. 9). Separation regions appeared over the surface of the roof tiles as the flow angle was gradually increased. The wind flow was along the surface of the roof at a lower pitch angle, whereas the flow was split directly by the surface and the edge of the roof tile at a higher pitch angle. The wind flow was toward the edge of the roof, and it was found that the flow became very turbulent locally over the edge and formed the separation regions. The appearance of the separation regions was considered to indicate a significant fall in the external pressure and a rise in the internal pressure, causing the fluttering of the roof tiles. The clattering of the model roof tiles was recognized in the Y-axis direction at a pitch angle of 29 degrees. It was found that this may be caused by the decrease of the critical velocity, which lifted up the tiles and caused them to flutter.

Figs. 6-8 show the results for several pitch angles. The largest number of roof tiles were buffeted and fluttered at the maximum pitch angle of 29 degrees (Fig. 6 (a)), resulting in three roof tiles being scattered. The roof tiles were not scattered at a pitch angle of 24 degrees (Fig. 7 (a)), whereas they were both buffeted and scattered at a pitch angle of 29 degrees. In this case, the roof tiles attached with the accelerometers and the eight neighboring roof tiles fluttered. At the minimum pitch angle of 19 degrees (Fig. 8 (a)), the roof tiles did not flutter even at the maximum velocity of 40 m/s, but a few roof tiles were buffeted.

Similarly, the signals from the accelerometers revealed fluttering at pitch angles of 24 and 29 degrees. The results obtained by the FFT analysis of the accelerometer signals at pitch angles of 24 and 29 degrees are shown in Figs. 7 (b) and 6 (b), respectively. The small-amplitude vibrations were recognized using accelerometers 1 and 2 at a low velocity at these pitch angles. However, a 50 m/s² vibration was recognized momentarily when the wind velocity was increased. The small-amplitude vibrations appeared at a low velocity, but gradually increased at a higher velocity (Peterka et al., 1997; Cermak, 1998). Moreover, acceleration and amplitude of the vibrations are related to the critical velocity at which fluttering occurs for a constant pitch angle of the roof. At a pitch angle of 24 degrees, the values of acceleration and amplitude increased when the wind velocity reached 40 m/s (Fig. 7 (b)). The acceleration and amplitude observed at a relatively high velocity for a pitch angle of 24 degrees also appeared at a low velocity for a pitch angle of 29 degrees (Fig. 6 (b)).

The maximum acceleration value prior to fluttering was found at pitch angles of 24 and 29 degrees. Moreover, it was found that the acceleration decreased when the roof tiles fluttered at both pitch angles. This was found to be caused by the balancing of internal pressure in the space between the attic side and the roofing board by the external pressure of the flow over the roof tiles. On the other hand, it was occasionally observed that the neighboring roof tiles touched each other and unexpected acceleration signals were found because of contact between neighboring roof tiles during vibration. The effects of the roof's pitch angle on their scattering were recognized by analyzing the acceleration signals.

In a series of wind tunnel tests, the pitch angles of the roof were changed and two accelerometers were attached to neighboring roof tiles in order to detect and analyze acceleration signals. Fig. 10 shows an example of the acceleration signals that were frequently found whenever small-amplitude vibrations occurred. It shows the acceleration

signals and the behavior of the 25 model roof tiles at a pitch angle of 24 degrees and wind flow of 40 m/s. In this experiment, it was also recognized that the tiles locally arranged at the back and right side of the roof were often buffeted and scattered by strong winds. In a typical construction method, tiles are piled up and laid on the upper and lower side of a roof by their own weight. Therefore, the roof tiles locally arranged at the back and right side of the roof are held by the relatively lighter weight of the neighboring roof tiles. The wave-forms shown for case A in Fig. 10 (a) indicate that the signals are out of synchronization by a half cycle from both accelerometers. The wave-forms shown for case B in Fig. 10 (b) indicate the nearly synchronized signals from both accelerometers. Fig.10 shows the time history of the acceleration signals caused by the wind effect. These results show that it was found that the accelerations and time histories of the two roof tiles differ from each other. The forces affected both roof tiles simultaneously. On the other hand, even when a force did not act directly on a roof tile, it affected the other roof tile. In this case, the roof tile equipped with accelerometer ① was held by the roof tile equipped with accelerometer ② and the force of the roof tile equipped with accelerometer ② was added, although the force of the roof tile equipped with accelerometer ① did not act directly on it. The force of the tile equipped with accelerometer ① was added to the roof tile equipped with accelerometer ② although the force of the roof tile equipped with accelerometer ② did not act directly on it (case A). It was observed during a series of experiments that the roof tiles were buffeted almost simultaneously when vibration occurred (case B).

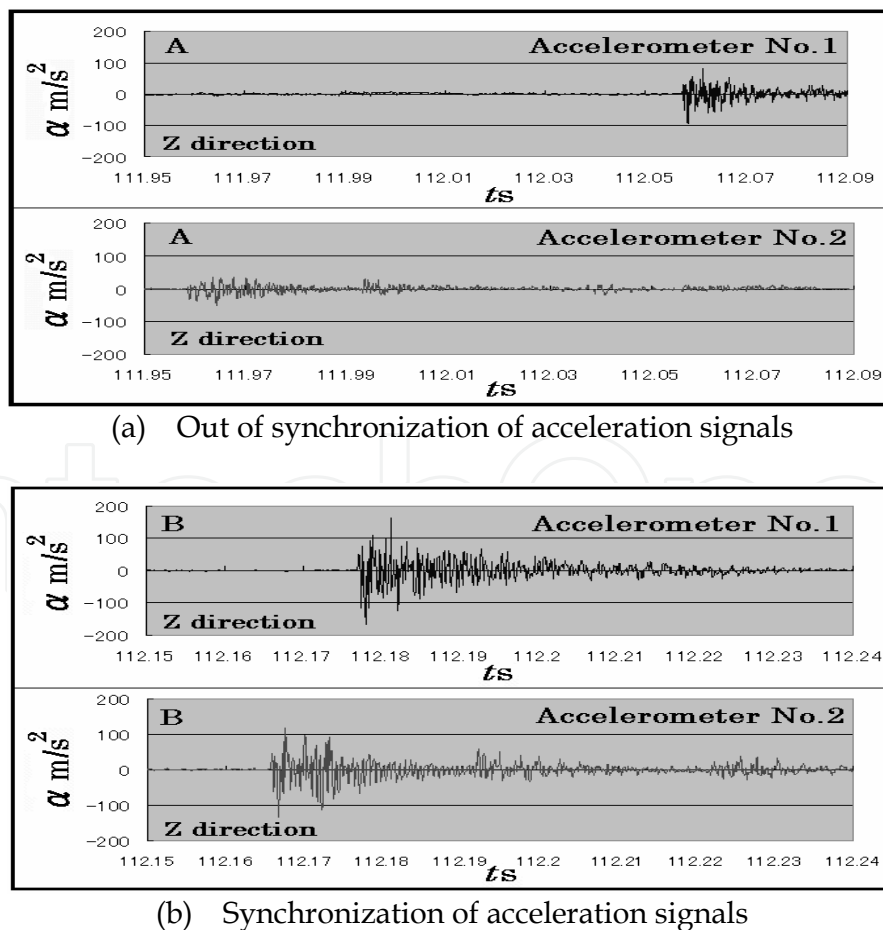


Fig. 10. Acceleration signals from accelerometers 1 and 2 at $\theta = 24$ degrees, $U = 40.0$ m/s

These results suggest that the roof tile held by the other roof tile was buffeted and then produced the reaction force on the neighboring roof tile. This behavior may be same as the “wave motion of roof tiles” phenomenon described by Ginger (2001), which is often reported to cause construction damage.

Hazelwood (1980b) described the lifting mechanism of a tile by a moment turning the tile upward around the pivoting point on the batten. The moment consists of a lifting force and two force couples caused by the external and internal pressure distributions, respectively. Fig. 11, which shows snapshots of a high-speed video camera picture, demonstrates this lifting mechanism for wind direction perpendicular to the eave. For a local flow direction perpendicular to the ridge, the internal pressure in the space between the tiles and underlay may become positive because of stagnation. As a result, the net wind load increases because of the sealing effect of the underlay. However, pressure equilibration in the gable roof is prevented, leading to a much lower net wind load for the leeward roof tiles. Aerodynamically favorable tiles should have a shape that prevents stagnation at the overlaps. The permeability at the overlapping gaps parallel to the ridge should be small and the permeability at the interlocking gaps perpendicular to the ridge, where suction occurs due to the element flow field, should be high (Hazelwood, 1980a).

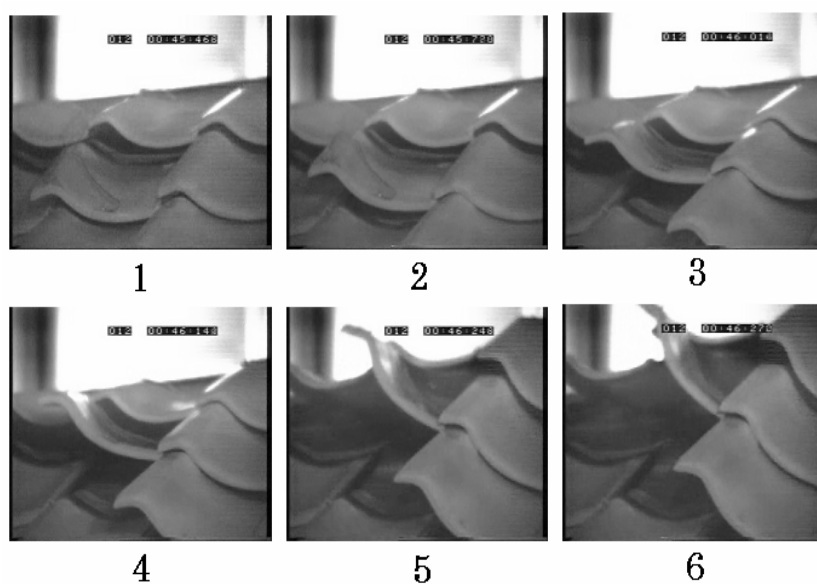
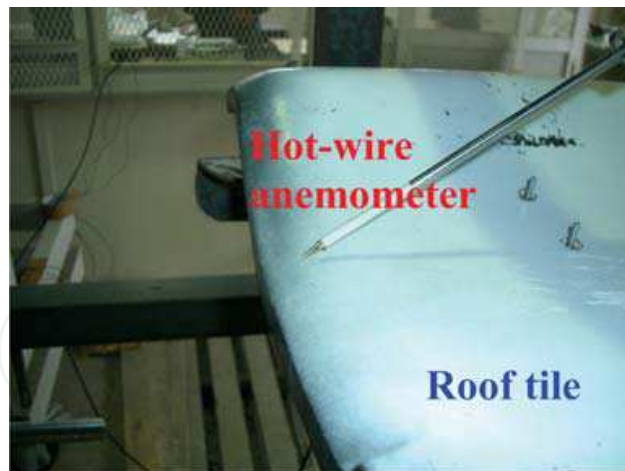


Fig. 11. Lifting up of roof tiles due to wind action as recorded by a high-speed video camera at $U = 40.0$ m/s

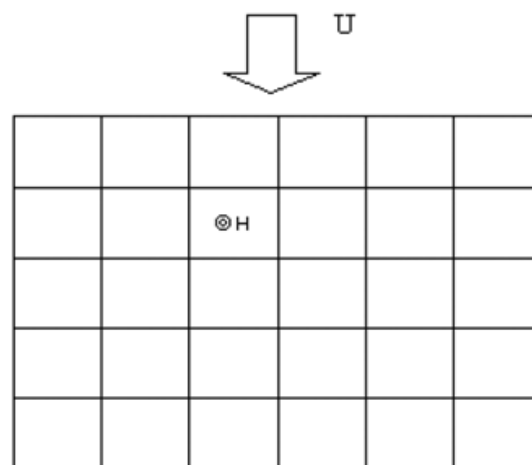
3.3 Transverse vibration of roof tiles

Fig. 12 shows an example of the typical turbulence spectrum obtained by the hot-wire anemometer for $\theta = 0$ degrees, $\phi = 90$ degrees, and $U = 40$ m/s. With a turbulence level of surface flow close to the roof tiles, the tiles exhibited only the typical turbulence-buffeting response within the intermediate ranges of the angle of incidence. The Reynolds number during the experiment was so high that the edge separation was turbulent. The sources of vibration are the front and side edge vortices (Fig. 13). The vibration amplitudes increased progressively with increasing velocity, which indicates a typical buffeting response.

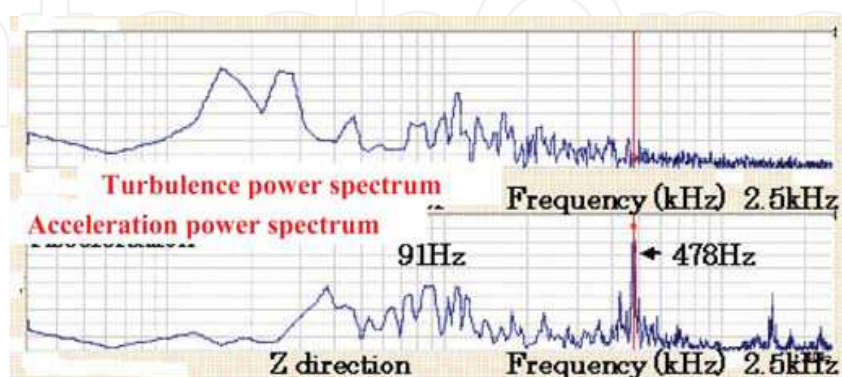


(a) Hot-wire anemometer and roof tile

⊙ Accelerometer
H Hot wire anemometer



(b) Positions of accelerometer and hot-wire anemometer



(c) Vibrational acceleration and turbulence power spectrum.

Fig. 12. Vibrational acceleration and turbulence power spectrum of roof tiles for $\theta = 0$ degrees, $\phi = 90$ degrees, and $U = 40.0$ m/s

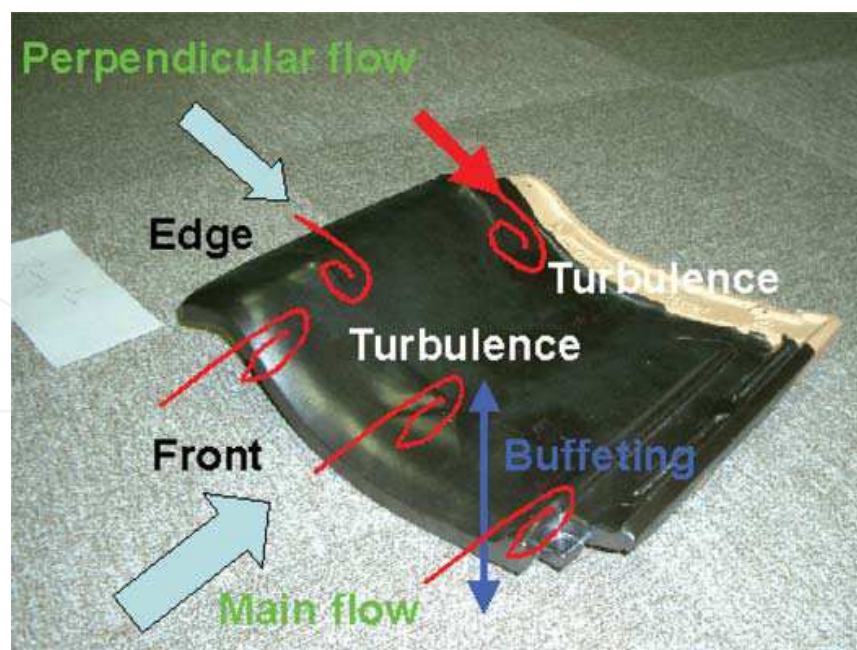


Fig. 13. Transverse vibration of roof tile

The local flow due to the outer shape of a surface element is of importance if the element is located in an area with attached flow, such as on the windward surface of a pitched roof. The gaps between the tiles may be exposed to local stagnation and/or suction depending on the shape of the tiles. If suction prevails, the internal pressure is decreased and the opposite takes place for predominating stagnation. For $\theta = 30$ degrees, a front edge vortex with its axis parallel to the ridge is formed, causing significantly higher negative pressure coefficients (Ginger, 2001). It is observed by the surface oil-flow visualization method that reattachment takes place upstream of the ridge and the flow is completely separated at the leeward roof area. If the roof pitch is increased, the vortex on the windward side decreases in size and reattachment takes place much closer to the eave. In the region of flow bifurcation, the pressure coefficient becomes positive (Peterka et al., 1997).

However, if the external pressure distribution is changed because of the shape of the element, the internal pressure can be affected significantly. In particular, for the local flow direction perpendicular to the ridge of a tiled roof, the flow is stagnated at the overlaps of the tiles. The stagnation pressure increases because of the step formed by overlapping tiles and leads to an increase in the internal pressure if the permeability of the overlap gaps is sufficient. This value depends on the shape of the front and side edges of the tile, i.e., square or round, and the level of free-stream turbulence; the larger the value of free-stream turbulence, the larger is the critical value of incidence. Because the pressure distribution on the roof is strongly influenced by the turbulence of the oncoming flow, this turbulence will also affect the net loading on roof elements.

If a roof tile is inclined with respect to the free stream, the flow will separate from one side as soon as the angle of incidence exceeds a critical value. Visualization using the surface oil flow method shows that the vortex cones caused by the yawing flow separation at the leading edges result in the highest negative pressure coefficients close to the windward gable and the windward eaves. If the roof pitch is increased, the vortex cones decrease in strength. In regions of separated flow, the external pressure distribution on a tiled surface

coincides with the pressure distribution on the roof surface, as described by Peterka et al. (1997). In regions of attached flow, however, the pressure distribution on a tile is influenced by the flow around the tile. A typical example for the change in the external pressure distribution due to the element flow field is shown in Hazelwood (1980a).

The pressure distribution, indicating an acceleration region at the eave-facing end of the tile and a stagnation zone in front of the overlap of the tile in the upper row, results in an upward-lifting moment. The predominant geometric parameter for the pressure distribution is the tile thickness related to the non-overlapping length (Peterka et al., 1997). The fluctuations of the surface flow velocity caused by the instabilities of the flow field over the roof will change the pressure distribution and make the tiles clatter. When the wind load exceeds a certain value, the tiles are lifted up and the permeability of the roof surface increases rapidly. If this happens in a region with low external pressure, the wind load on the tiles will decrease. However, if lifting-up occurs because of surface flow action on the windward side, the stagnation effect will lead to an increase in the internal pressure and the up-lifting tile load. The internal pressure underneath the tiles affects the overall stability of the tiles and acts as the up-lifting tile load.

The small-amplitude vibrations of the roof tiles appeared first, the amplitude grew gradually larger as the wind velocity increased, and then fluttering with large-amplitude vibrations occurred, finally followed by scattering. The vibrational frequency was identified by image analysis of the high-speed video camera to measure relatively high-amplitude vibration in fluttering, which is considered to be the direct cause of tile scattering. The roof tiles do not always oscillate with a fixed vibrational frequency. Because vibrations with several frequencies affected the tiles and showed complex behaviors, some oscillation patterns were chosen at random from the data to be analyzed further. It was found that the amplitudes of tile vibration were larger than that of their natural frequency, and the vibration frequencies were low (in the range of 10 - 20 Hz).

The results obtained by the FFT analysis of the acceleration signals in the experiment in which fluttering occurred are shown in Fig. 14. The results show the oscillation of fluttering at a pitch angle of 24 degrees and a wind velocity of 40 m/s. The wind velocity was gradually increased from the start of the wind tunnel test to its maximum velocity, and the acceleration measurement and the video camera recording were then started simultaneously. The sampling time of the FFT analyzer was set at 2,048 points, the frequency resolution was set at 800 lines, and the frequency range was 0 - 5 kHz. Moreover, the peak frequency of approximately 470 Hz, which appeared just before tile scattering, was the natural frequency and was also recognized by FFT analysis. To minimize the effects of sampling time on the results of the FFT frequency analysis, the FFT frequency was analyzed using a sufficient sampling time. As a result the relatively high frequency, i.e., the natural frequency, as well as the relatively low frequencies were recognized.

It was observed in the wind tunnel test that the bolted roof tiles were lifted up, damaged, and then scattered by the wind, and they induced further fluttering and clattering by lifting up their neighboring roof tiles. In other words, it is believed that the amplitude was the largest in one cycle of tile vibration and the largest energy was obtained at those moments. The force acting on the roof tile can be estimated by Newton's second law of motion. In the case of the measured acceleration of 11 m/s^2 and the given mass of 2.8 kg, the force acting on the roof tile was 30.8 N.

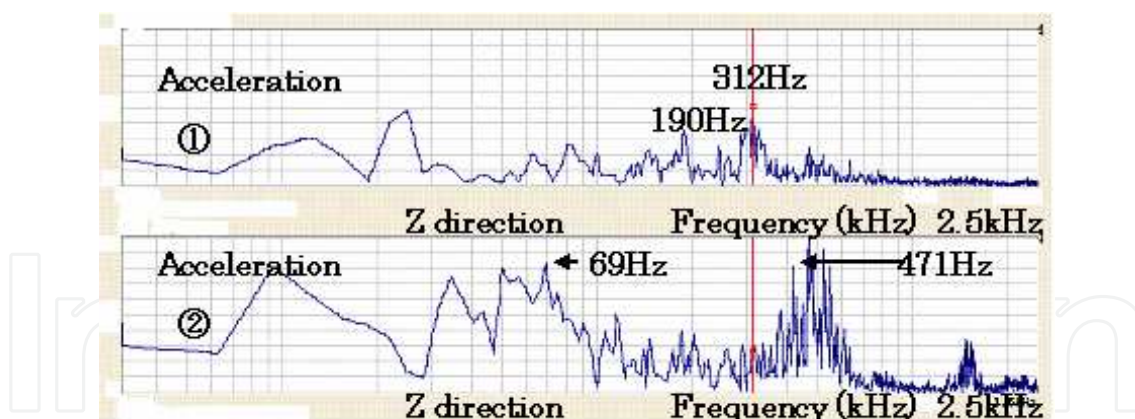


Fig. 14. Vibrational acceleration power spectrum of roof tiles at $\theta = 24$ degrees, $U = 40.0$ m/s

The natural frequency of the roof tile was measured by the impulse force hammer test. The center of a roof tile hung from the ceiling was hit by the impulse hammer. The natural frequency of the tile was analyzed in terms of a frequency-response function and a coherence function. By analyzing the frequency-response function, the peak frequency was found to be 478 Hz. The coherence function was strongly correlated with the frequency-response function (Fig. 5 (b)). It was recognized that the dominant frequency, which occurred just before the scattering shown in Fig. 14, almost coincided with the natural frequency of the tiles that was found by the impulse force hammer test. The natural frequencies of the roof tile hung from the ceiling were found to be between 430 and 460 Hz. The peak frequency of the roof tile appeared just before scattering, as shown in Fig. 14. The roof tiles were arranged on the model roof in order to measure their vibrational frequency caused by the wind at the center of the opposite side of the roof. It was found that the measured frequency was different from the frequency of fluttering and the natural frequency of the tiles (Naudascher et al., 1993; Hazelwood, 1980b).

These test results showed that the vibrational frequency of about 14 Hz almost coincided with the vibrational frequency that was obtained by analyzing the images of the high-speed video camera. On the other hand, the information of the acceleration and the results of the image were analyzed to specify the vibration occurring during fluttering. Low-frequency vibrations (10 - 20 Hz) were detected first (Fig. 14). Next, the significant peak amplitude of the natural frequency, which appeared just before fluttering, was also recognized. In other words, it is believed that the vibration at the relatively low frequency has a dominant effect on fluttering, and this natural frequency appears prior to fluttering because of the significant vibration at the relatively high natural frequency just before fluttering. Finally, the occurrence of vibration at the low frequency with a relatively large amplitude has the greatest effect on fluttering, and this mechanism can result in the lifting of the roof tiles. Hence, the dynamics of the roof tiles were due to the balance of their own weight, to which the external pressure was added by the fluid over the surface of the roof, and the internal pressure (i.e., the space between the roof tile and the roofing board). Because the external pressure and the internal pressure were changed, an unbalance of both pressures occurred, the tiles became unstable, and then fluttering occurred. It is believed that the relatively low-frequency vibrations have the greatest effect on scattering and can be the main factor that controls the behavior of the roof tiles.

4. Future research

Strong winds not only result in tile scattering leading to damage of tiles, but also result in water leak damage. Experiments pertaining to water leaks can be broadly classified into pressure box-type experiments and blower/water dispersion-type experiments. Pressure box-type experiments allow for the recreation of model wind pressures using devices for either increasing or decreasing pressure. Conversely, blower/water dispersion-type experiments make use of devices consisting of blowers and water dispersion equipment, which allow experiments to be conducted in conditions very similar to the actual flow of wind and rain during stormy weather. However, these types have both advantages and disadvantages, and neither of these types is able to reproduce the actual conditions of both rain damage and the damage caused by heavy winds simultaneously.

In future work, the authors will focus their attention on vibrations which cause the preliminary phenomena eventually leading to the scattering of tiles due to the effects of the wind, and will seek to understand the mechanism of these vibrations. Consequently, the authors will be able to connect together the mechanism and the preliminary phenomena of the occurrence of tile vibration induced by fluid flow. In accordance with these results, in future work the authors will go beyond the conventional understanding of water leakage amounts, aiming to establish appropriate experimental methods and to clarify the mechanism underlying the occurrence of water leak phenomena. The authors intend to investigate the previously unknown influence exerted by tile vibrations on water leaks. The ultimate goals are to provide a conclusive understanding of the effects of wind and to provide suggestions for possible improvement and redesign of roof tiles (Fig. 15).

5. Conclusions

An experimental study was conducted using wind tunnel tests in order to explain the behavior of roof tile vibration and the primary factors that affect scattering. The results are summarized as follows.

1. The basic mechanism that can lead to flow-induced vibrations of roof tiles is similar to that of the so-called fluttering instability, which appears as self-excited oscillations in the natural mode of a structure at a certain critical flow speed. The oscillating frequencies are related to the natural frequencies of vibration.
2. Surface flow is only important on the windward side of a roof and creates reasonable up-lifting moments only for wind directions roughly perpendicular to the eaves.
3. The effects of a roof's pitch angle on the fluttering of roof tiles were confirmed by analyzing acceleration information as the pitch angle was increased; the absolute value of acceleration and the amplitude also increased with increasing pitch angle.
4. The "wave motion of roof tiles" appeared just before scattering was observed, and the forces acting on two neighboring roof tiles were found to be either synchronized or out of phase.
5. Low-frequency vibrations, which have the greatest effect on scattering, were identified by a high-speed video camera, and the major factor that controls the behavior of the roof tiles was found to be the balance between the external pressure and the internal pressure.

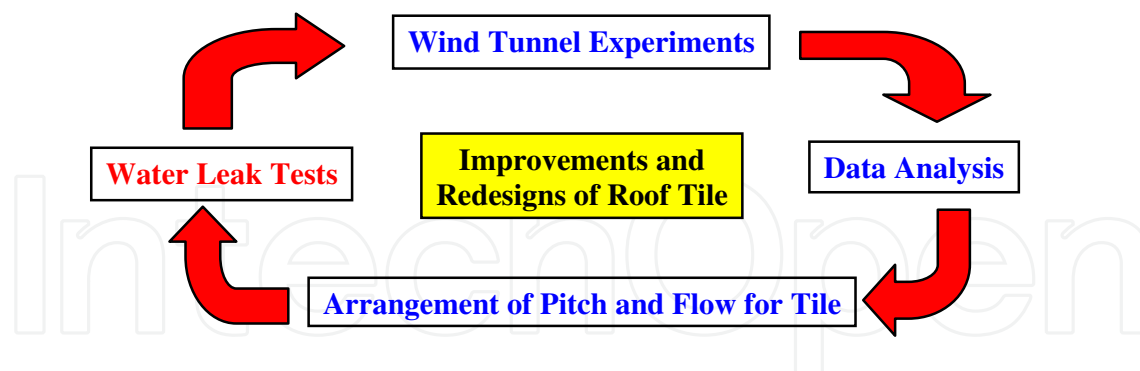


Fig. 15. Research plan for future work.

6. Acknowledgments

We wish to thank Dr. R. Nanba, Mr. K. Shibao, Mr. M. Satou and Mr. Y. Shibao of Shibao Co. Ltd. for their guidance in planning the present work. We also wish to thank the staff of Shimane Institute for Industrial Technology for their assistance. This work was supported by Grant-in-Aid for Scientific Research (C) of Japan Society for the Promotion of Science.

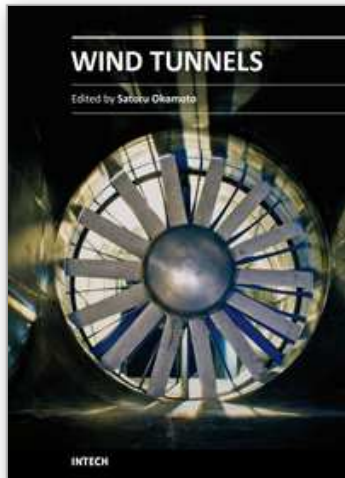
7. References

- Cermak, J. E. (1998). Wind damage mitigation - Wind engineering challenges, In: *Wind Effects on Buildings and Structures*, Riera, J. D. & Davenport, A. G. (Eds.), pp. 335-352, A. A. Balkema, 9054109599, Rotterdam.
- Ginger, J. D. (2001). Characteristics of wind loads on roof cladding and fixings. *Wind and Structures*, Vol.4, No.1, pp. 73-84.
- Hazelwood, R. A. (1980a). Principles of wind loading on tiled roofs and their application in the British standard BS5534. *Journal of Wind Engineering and Industrial Aerodynamics*, Vol.6 (July 1980) pp. 113-124, 0167-6105.
- Hazelwood, R. A. (1980b). The interaction of the principal wind forces on roof tiles, *Proceedings of 4th Coll. Industrial Aerodynamics, part1*, pp. 119-130, Aachen, 1980.
- Kramer, C., Gerhardt, H. J. & Kuster, H. W. (1979). On the wind-loading mechanism of roofing elements. *Journal of Wind Engineering and Industrial Aerodynamics*, Vol.4 (August 1979) pp. 415-427, 0167-6105.
- Kramer, C. & Gerhardt, H. J. (1983). Wind loads on permeable roofing systems. *Journal of Wind Engineering and Industrial Aerodynamics*, Vol.13 (December 1983) pp. 347-358, 0167-6105.
- Naudascher, E. & Wang, Y. (1993). Flow-induced vibrations of prismatic bodies and grids of prisms. *Journal of Fluids and Structures*, Vol.7, Issue 4 (May 1993) pp. 341-373, 0889-9746.

Peterka, J. A., Cermak, J. E., Cochran, L. S., Cochran, B. C., Hosoya, N., Derickson, R. G., Harper, C., Jones, J. & Metz, B. (1997). Wind uplift model for asphalt shingles. *Journal of Architectural Engineering*, (December 1997) pp. 147-155.

IntechOpen

IntechOpen



Wind Tunnels

Edited by Prof. Satoru Okamoto

ISBN 978-953-307-295-1

Hard cover, 136 pages

Publisher InTech

Published online 10, February, 2011

Published in print edition February, 2011

Although great advances in computational methods have been made in recent years, wind tunnel tests remain essential for obtaining the full range of data required to guide detailed design decisions for various practical engineering problems. This book collects original and innovative research studies on recent applications in wind tunnel tests, exhibiting various investigation directions and providing a bird's eye view on this broad subject area. It is composed of seven chapters that have been grouped in two major parts. The first part of the book (chapters 1–4) deals with wind tunnel technologies and devices. The second part (chapters 5–7) deals with the latest applications of wind tunnel testing. The text is addressed not only to researchers but also to professional engineers, engineering lecturers, and students seeking to gain better understanding of the current status of wind tunnels. Through its seven chapters, the reader will have an access to a wide range of works related to wind tunnel testing.

How to reference

In order to correctly reference this scholarly work, feel free to copy and paste the following:

Satoru Okamoto (2011). Experimental Study of Flow-Induced Vibrations and Scattering of Roof Tiles by Wind Tunnel Testing, *Wind Tunnels*, Prof. Satoru Okamoto (Ed.), ISBN: 978-953-307-295-1, InTech, Available from: <http://www.intechopen.com/books/wind-tunnels/experimental-study-of-flow-induced-vibrations-and-scattering-of-roof-tiles-by-wind-tunnel-testing>

INTECH
open science | open minds

InTech Europe

University Campus STeP Ri
Slavka Krautzeka 83/A
51000 Rijeka, Croatia
Phone: +385 (51) 770 447
Fax: +385 (51) 686 166
www.intechopen.com

InTech China

Unit 405, Office Block, Hotel Equatorial Shanghai
No.65, Yan An Road (West), Shanghai, 200040, China
中国上海市延安西路65号上海国际贵都大饭店办公楼405单元
Phone: +86-21-62489820
Fax: +86-21-62489821

© 2011 The Author(s). Licensee IntechOpen. This chapter is distributed under the terms of the [Creative Commons Attribution-NonCommercial-ShareAlike-3.0 License](#), which permits use, distribution and reproduction for non-commercial purposes, provided the original is properly cited and derivative works building on this content are distributed under the same license.

IntechOpen

IntechOpen